Structural and dielectric properties of Bi doped $Ba_{0.6}Sr_{0.4}TiO_3$ ceramics

Wei Chen · Xi Yao · Xiaoyong Wei

Abstract The dielectric properties of 0.1–15% mol bismuth doped $Ba_{0.6}Sr_{0.4}TiO_3$ (BST) ceramics have been investigated systematically. The solubility limit of bismuth is determined as about 10 mol% by means of both X-ray diffraction and scanning electron microscopy, which is further verified by the fact that the lattice constant of the samples above 10 mol% is almost invariable. The temperature dependence of the dielectric permittivity suggest that the ferroelectric behavior transit to relaxor ferroelectric type when impurity concentration reaches 5 mol%, and further to relaxor behavior for samples above 10 mol% Bi content, which is verified by the absence of a hysteresis loop. Thermal expansion results show differences between 5 and 10 mol% doped samples. Dielectric tunability at room temperature decreases with bismuth content increasing. The variation of properties was attributed to the impurity induced polar regions and former long-order structure.

Introduction

Barium strontium titanate (BST) ferroelectric materials have shown great promise for application as the phase shifting elements in phased array antennas and as tuning elements in devices operating at microwave frequencies because of its high tunability and low dielectric losses [1, 2]. It has also been investigated with considerable interest as a dielectric material for future-generation dynamic random access memories [3], and infrared detectors based on uncooled focal plane arrays [4, 5]. For improving the material performance for the use in tunable devices, many efforts have been made in the doping. Some dopants including Mg^{2+}, Mn^{2+}, Al^{3+}, Co^{3+}, Ni^{2+}, Fe^{3+}, which can occupy the B sites of the ABO_3 perovskite structure and behave as electron acceptors, have been known to lower the dielectric loss [6–11]. Other papers reported the effect of dopants which can occupy the A sites of the perovskite structure on the properties of BST, such as K^+, La^{3+}, and Er^{3+} [12–14]. However, few papers reported the effect of Bi impurity for BST ceramics. Zhou et al. [15] suggested that Bi^{3+} can substitute Sr^{2+} and act as a donor in the A sites of the BST perovskite structure, then off-center Bi^{3+} ions and Bi^{3+}-V_A'' centers form dipoles and thus set up local electric fields, which suppress the ferroelectric of solid solution and result in the relaxor behavior. In our previous report [16], 5 mol% Bi doped BST demonstrated this point, meanwhile, Yun and Wang [17] had also the same view of points to this in Bi doped (Ba,Ca)-TiO_3 system.

Considering dielectric behavior, the contrast between normal ferroelectrics (FEs) and relaxors is listed by Samara [18]. Because of the impurity in ABO_3 perovskites, dipolar entities form polar nanodomains whose size is determined by the dipolar correlation length, r_c, and exhibit dielectric relaxation under an applied ac field. In the very dilute limit each domain behaves as a non-interacting polar entity with a single relaxation time. At higher concentrations of disorder, however, the domains can interact leading to a more complex relaxation behavior. Among the manifestations of such behavior is the formation of a glass-like relaxor state, or even an ordered ferroelectric state for a sufficiently high concentration of overlapping domains.

W. Chen (✉) · X. Yao · X. Wei
Electronic Materials Research Laboratory, Key Laboratory of the Ministry of Education, Xi'an Jiaotong University, Xi'an 710049, P.R. China
e-mail: lffwster@gmail.com

In this article, we present systematic studies of the effect of Bi addition into $Ba_{0.6}Sr_{0.4}TiO_3$ (BST) ferroelectrics on the microstructure and dielectric properties of Bi-mixed BST materials, with emphasis on the different dielectric behavior for different Bi concentration. In particular, an extensive view based on Samara's is proposed about the transition from a ferroelectric to relaxor, which is attributed to the interaction between the impurity induced polar regions and former long-order structure.

Experimental procedure

The polycrystalline $(Ba_{0.6}Sr_{0.4})_{1-1.5x}Bi_xTiO_3$ ceramics ($0 \leq x \leq 0.20$) were obtained from conventional mixed-oxide powder. High-purity $BaCO_3$, $SrCO_3$, TiO_2, and Bi_2O_3 powders were mixed for 6 h by ball milling in distilled water. The powders were calcined at 1,100 °C for 6 h. After calcination, the powders were pressed at 20 MPa into disks and sintered in a range of 1,380–1,195 °C in air for 4 h and furnace cooled. The X-ray powder diffraction (XRD) was carried out using an X-ray diffractometer (2400, Rigaku, CuK_α radiation). The microstructure of the samples was observed in unpolished sections, using scanning electron microscopy (JSM-5800, JEOL).

For dielectric measurements, sintered samples were polished and covered with silver electrodes on both sides. The dielectric permittivity of the samples was measured using an HP4284 LCR meter from 100 Hz to 1 MHz in a temperature range of –190 to 50°C at a rate of 1 °C/min. The hysteresis loops were measured by a TF analyzer 2000 FE-module system (AIXACCT). The dielectric tunability was measured using a dc power source (PS350/5000V-25W) and a multi-frequency LCR meter (TH2816) at room temperature.

Crystalline structure, microstructure, and lattice parameter

Crystalline structure and phase

The XRD patterns of Bi doped BST ceramics are shown in Fig. 1. The ceramics showed single cubic perovskite phase when $x \leq 0.10$. Slight change in the 2θ angles in comparison with pure BST solid solution was observed, indicating that some Bi ions entered into the BST lattice. When Bi concentration is above 0.10, a second phase appears which is believed to be $Bi_4Ti_3O_{12}$.

Microstructure

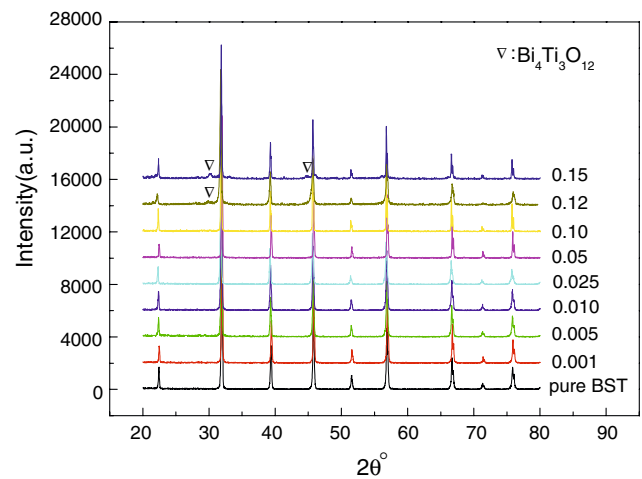SEM images of samples from $x = 0.01$ to $x = 0.20$ are shown in Fig. 2. Dense and homogeneous grain structure

Fig. 1 The XRD patterns of all compositions in $(Ba_{0.6}Sr_{0.4})_{1-1.5x}Bi_xTiO_3$ ceramics

was found for the compositions with $x = 0.10$. The crystalline boundary became ambiguous for the sample of $x = 0.10$, and a sheet-like second phase was segregated when $x = 0.12$. This phase became gradually evident and excessive with Bi increasing. This result, which well in agreement with that of the XRD suggests that the solubility limit of bismuth is about 10 mol%.

Lattice parameter

The lattice parameter of the $(Ba_{0.6}Sr_{0.4})_{1-1.5x}Bi_xTiO_3$ solid solutions with $0 \leq x \leq 0.15$ was measured by outer standard method and was calculated using the least square approach. The lattice parameter as a function of Bi content is shown in Fig. 3. The lattice parameter of the samples below 10 mol% increases linearly with increasing Bi concentration, and above 10 mol% the lattice parameter is nearly invariable. The result further confirms that the solubility limit of this system is 10 mol%.

Dielectric properties and discussion

Dielectric behavior

The temperature dependence of the dielectric constant for all the $(Ba_{0.6}Sr_{0.4})_{1-1.5x}Bi_xTiO_3$ compositions at 10 kHz is shown in Fig. 4. The effects of Bi doping on the permittivity can be clearly seen from this picture. The Curie temperature (T_c) shifts to lower temperatures, from 8.5 °C for undoped BST to –51 °C for 5 mol% Bi doped BST, and the transitions at T_c becomes more diffused as Bi-doping content increases until the Bi content reaches 5 mol%. When the Bi-doping content is above 5 mol%, the

Fig. 2 SEM micrographs of $x = 0.01$ (**a**), $x = 0.05$ (**b**), $x = 0.10$ (**c**), $x = 0.12$ (**d**), $x = 0.15$ (**e**), and $x = 0.20$ (**f**) in $(Ba_{0.6}Sr_{0.4})_{1-1.5x}Bi_xTiO_3$ ceramics
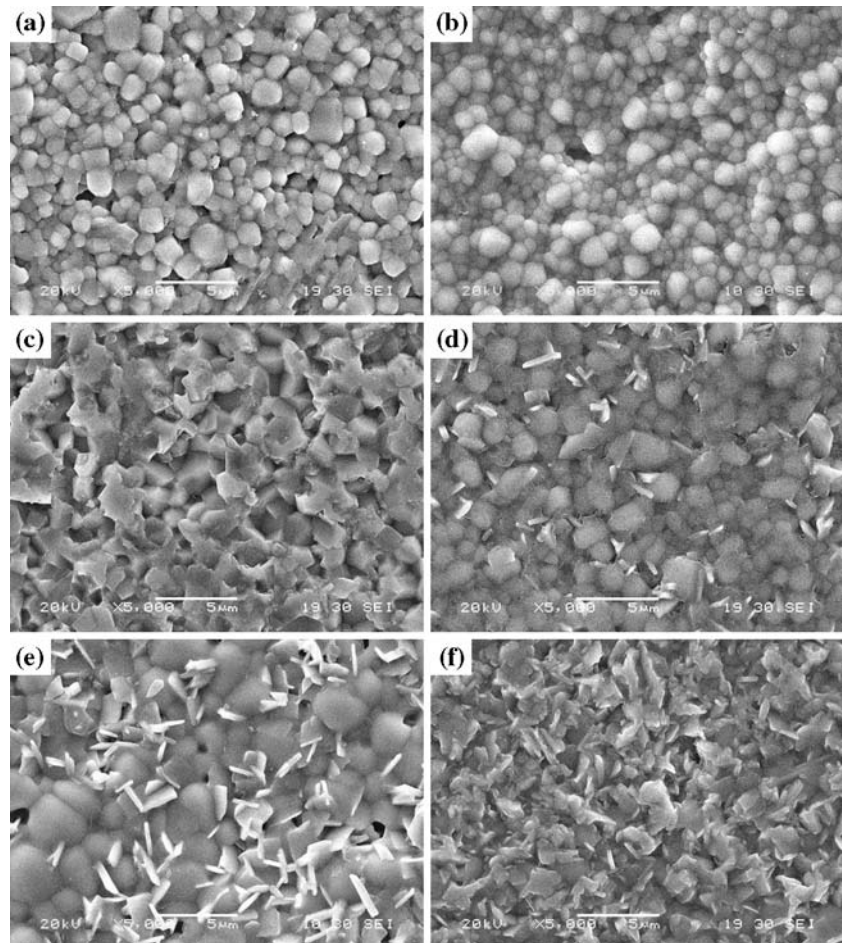
permittivity over the whole temperature range decreases without further shift in peak temperature, and the peak became more diffused. Meanwhile, the overall losses of the BST ceramics are significantly suppressed as the Bi concentration increases, as can be seen from Fig. 5. Figure 5 shows plots of ε and $\tan \delta$ versus T at different frequencies
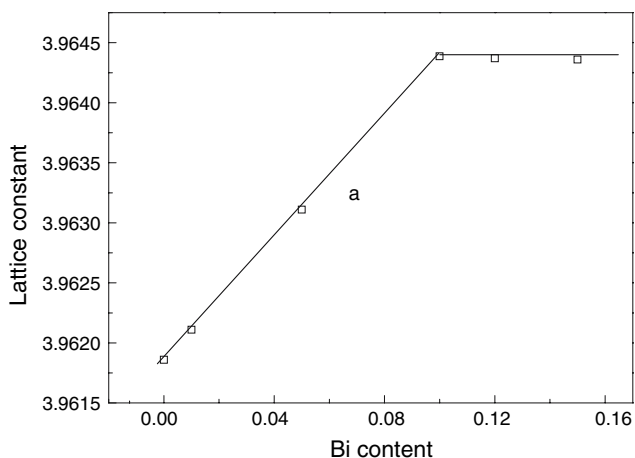

Fig. 3 Lattice parameters for all compositions of this system

for some typical compositions with $x = 0, 0.001, 0.05$, and 0.10. It can be seen that for different Bi doping concentrations, the sample exhibit different dielectric behavior. In nominally pure BST ceramics, the dielectric responses show that there are three frequency independent dielectric peaks A, B, and C, which are related to the successive ferroelectric phase transitions (Rhombohedral-Orthorhombic, Orthorhombic-Tetragonal, and Tetragonal-Cubic), respectively [15]. When 0.1 mol% Bi was introduced, the peak at the lowest temperature disappeared and the other two peaks became diffused. For the sample with $x = 0.05$, only one peak is left, which is apparently diffused and frequency dependent, a typical character of relaxor ferroelectrics. As for the sample with $x = 0.10$, the peak becomes more diffused and frequency dependent, relaxor behavior is dominant. For a doped system, the loss above maximum temperature (T_m) also decreases gradually from around 0.05 (0.1 mol% Bi) to about 0.002 as the Bi content increases up to 10 mol%.

The frequency dispersion of permittivity and an obvious departure from the Curie-Weiss law observed in Fig. 5d, suggests a relaxor-type behavior for the sample with high Bi content. The diffuseness of the phase transition can be
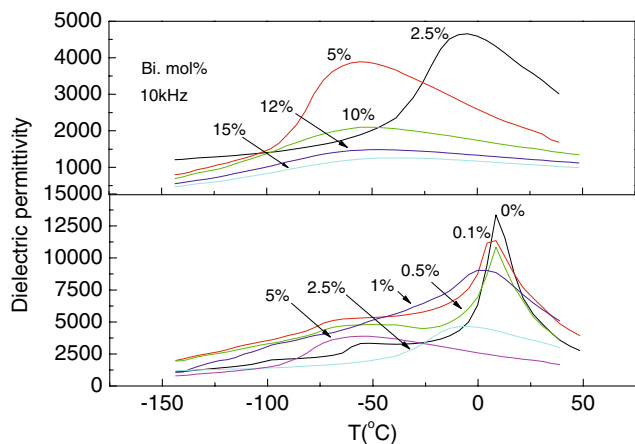
Fig. 4 Dielectric permittivity (at 10 kHz) of $Ba_{0.6}Sr_{0.4}TiO_3$ ceramics with different Bi-doping concentrations

described by an empirical parameter ΔT, defined as the difference between $T_{0.9\varepsilon_m(100Hz)}$ (the temperature corresponding to 90% of the permittivity maximum (ε_m) on the high-temperature side) and $T_{\varepsilon_m(100Hz)}$, i.e., $\Delta T = T_{0.9\varepsilon_m(100Hz)} - T_{\varepsilon_m(100Hz)}$. Another parameter ΔT^* adopted to quantify the degree of relaxation behavior is defined as $\Delta T^* = T_{\varepsilon_m(100kHz)} - T_{\varepsilon_m(100Hz)}$. The ΔT and ΔT^* parameters obtained are illustrated in Fig. 6. It can be seen from it, for the samples with low x, that both values are small, implying close to normal ferroelectric behavior. With an increase in Bi content, the two parameters increase quickly, implying that the system is becoming more relaxor like.

Hysteresis loops

The hysteresis loops for the samples of $x = 0$, $x = 0.05$, $x = 0.10$ are shown in Fig. 7. It can be seen that there is a typical hysteresis loop for composition $x = 0$, and only a slight change exists for different temperatures. The hysteresis loop for $x = 0.05$ became more broad and saturated with decreasing temperature. For the sample with $x = 0.10$, there is a lossy loop near maximum temperature (T_m) instead of a ferroelectric hysteresis loop. Furthermore, for higher and lower temperatures, only straight-line type loops were founded. Accordingly, the ferroelectricity of this sample was drastically weakened. What we can conclude from this experiment is: with Bi concentration increasing, the sample of pure BST transited from classical ferroelectrics to relaxor ferroelectrics ($x = 0.05$), then to non-ferroelectric relaxor behavior ($x = 0.10$).

Thermal expansion

The thermal expansion data $S_T(T)$ shown in Fig. 8a were measured for the 5 mol% BST and 10 mol% BST, and are
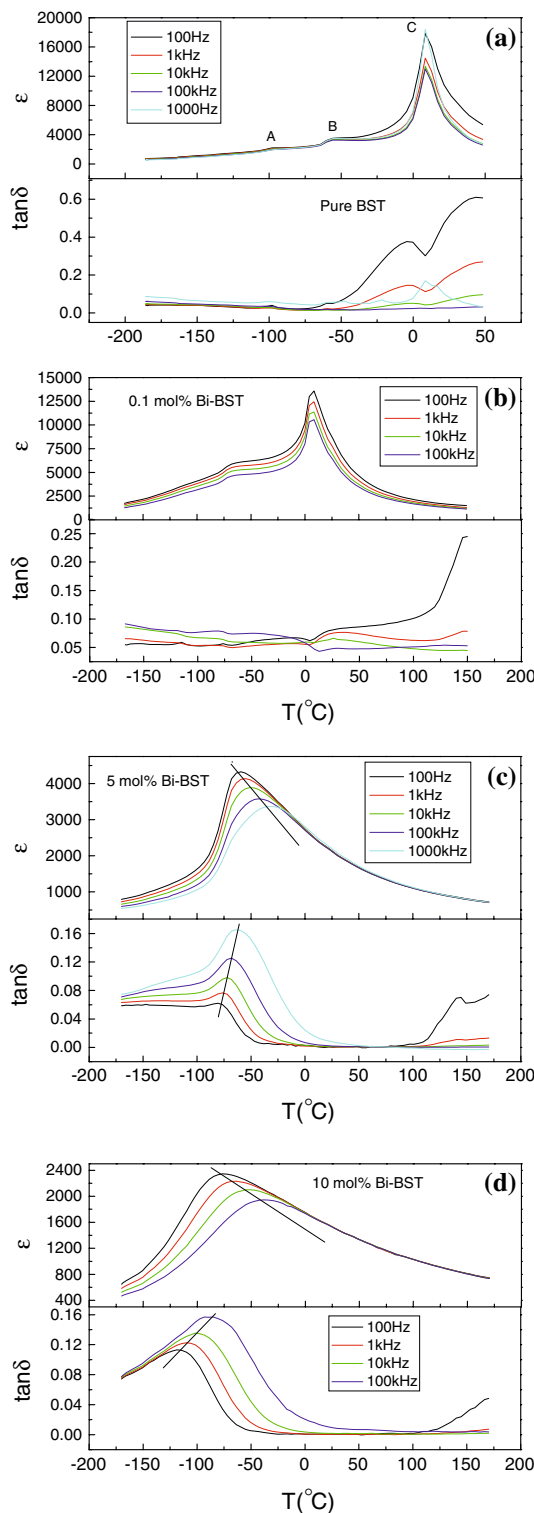

Fig. 5 Dielectric properties at different frequencies for the compositions of $x = 0$ (**a**), $x = 0.001$ (**b**), $x = 0.05$ (**c**), and $x = 0.10$ (**d**)

similar to previous results [19, 20]. It can be seen from this picture that both curves exhibit non-linear character, and a shoulder appears around –51 °C (also the phase transition
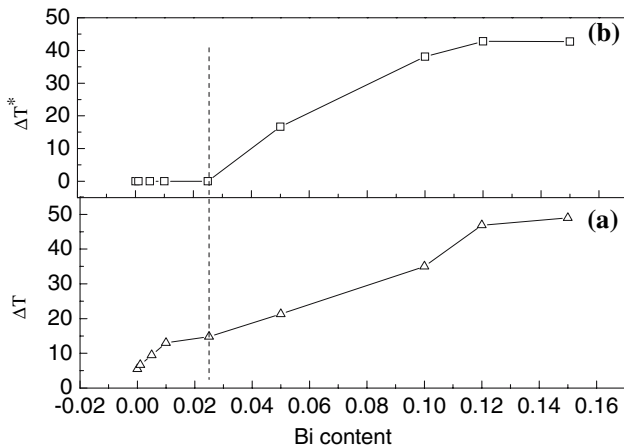
Fig. 6 Diffusion degree (**a**) and Relaxation degree (**b**) as a function of Bi content

temperature) for the 5 mol% Bi doped BST. However, there is no such trait for the 10 mol% BST sample. Thermal expansion coefficients $\alpha(T) = S_T(T)/dT$ shown in Fig. 8b, which were determined from the experimental data for $S_T(T)$. At high temperatures, $\alpha(T)$ shows nearly linear temperature dependence, both in 5 mol% BST and 10 mol% BST. Upon further cooling, the temperature dependence changes in 5 mol% BST and $\alpha(T)$ starts to decrease more steeply and subsequently increases. The anomaly in 5 mol% BST should be ascribed to the polar nanoregions being the precursor of the ferroelectric phase transition at –51 °C [21], whereas, the fact that there is no such anomaly around the dielectric peak temperature in 10 mol% BST demonstrated that the dielectric peak of this sample was not a phase transition peak. So the sample of 10 mol% BST was more inclined to show relaxor like behavior.

Dielectric tunability

The tunability, which is defined as $(\varepsilon_0 - \varepsilon_V)/\varepsilon_0 \times 100\%$, where ε_0 and ε_v denote permittivity without and with dc bias voltage, respectively, has been measured at room temperature for the Bi doped BST ceramics in the paraelectric region (Fig. 9). The results clearly show that the tunability decreases remarkably as the doped Bi content increases till 5 mol%, and slightly from 5 to 10 mol%. And the tunability is nearly invariable above 10 mol%. Because of the low losses in the Bi doped BST ceramics as shown in Fig. 5, the figures of merit (defined as tunability/loss [22]) are much higher than that of undoped BST ceramics, which makes Bi doped BST ceramics attractive materials for tunable microwave applications.
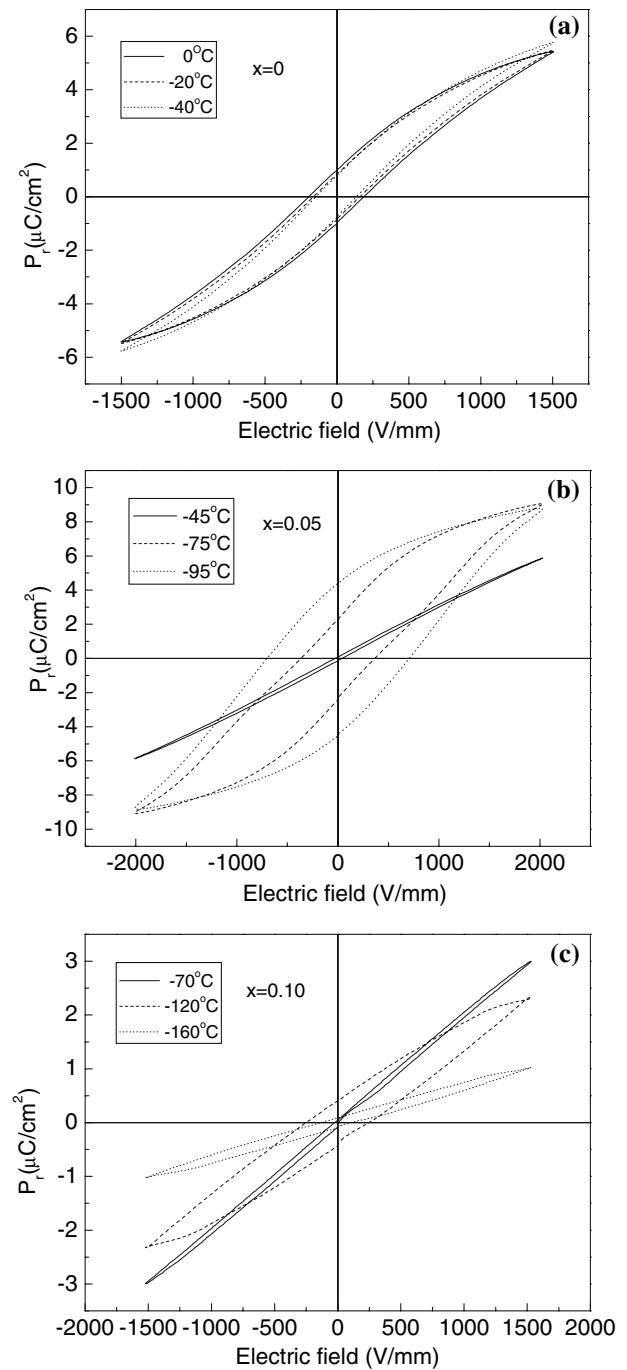
Fig. 7 Hysteresis loops for the compositions of $x = 0$ (**a**), 0.05 (**b**), and 0.10 (**c**) at 1 Hz

Discussion

From the above results, we can learn that there are three kinds of dielectric mechanisms. For Bi content below 1 mol%, the dielectric behavior of the samples suggested an evident diffused behavior differed from pure BST. The ferroelectric behavior is slightly weakened, which is attributed to the impurity induced long-range order
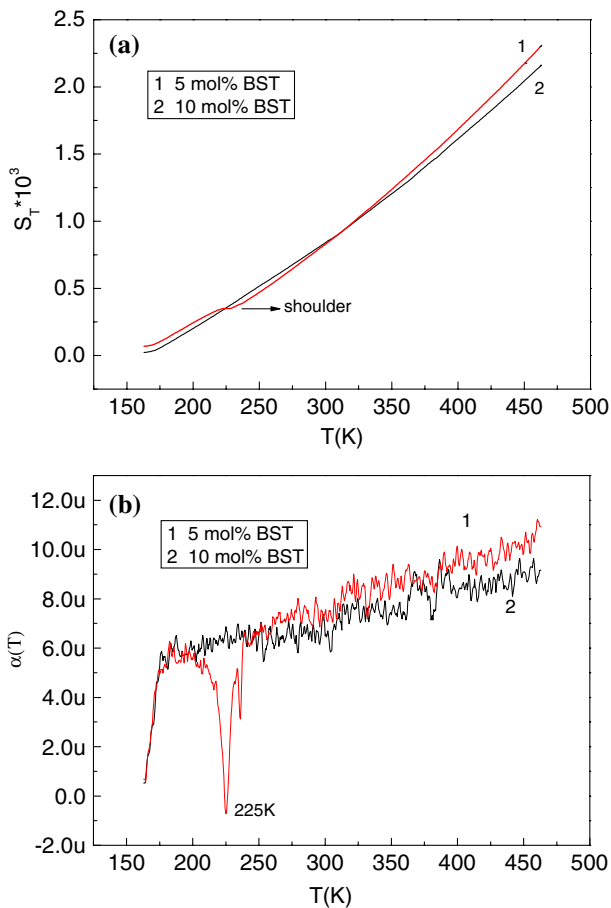
Fig. 8 Thermal expansion (**a**) and thermal expansion coefficient (**b**) of BST-5 and BST-10

Fig. 9 Room-temperature tunability as a function of Bi content

destruction. According to the reports [15, 16], Bi^{3+} ions substitutions for Sr^{2+} in BST ceramics can be located at off-center positions and A-site vacancies (V_A'') also appear to compensate the charge imbalance arising from the substitution of A-sites by Bi^{3+} ions, then $Bi^{3+} - V_A''$ dipolar defect was formed. These dipoles are dispersing at random locations in the host lattice, which form polar nanoregions, and finally play a destructive role in the primary long-range order structure.

With increasing Bi^{3+} concentration, the ferroelectric long-range order was further destructed by the impurity, while at the same time, the concentration of impurity induced polar nanoregions increased. The interactions among these regions become remarkable. It is the competition between long-range order and impurity induced polar region that determines the relaxor ferroelectric dielectric behavior for samples from 1 to 10 mol%. The relaxor behavior becomes more evident and ferroelectric behavior is more weakened with Bi content increasing. Relaxation phenomenon observed in the sample with $x = 0.05$ particularly indicates that at this composition the material is a
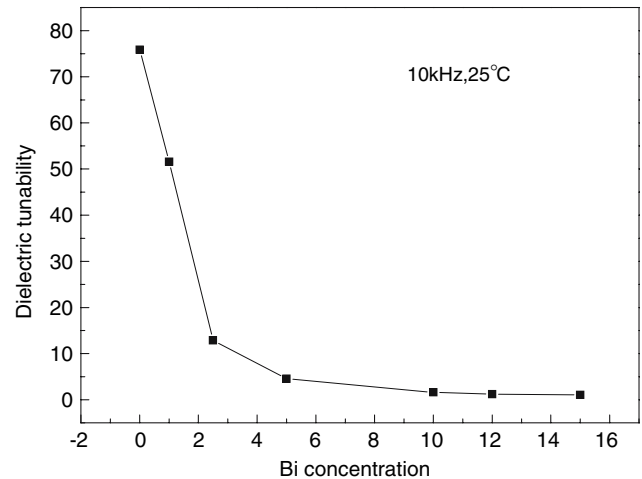
relaxation ferroelectric [16]. This assertion is further supported by the characterization of the corresponding hysteresis loops, i.e., evolvement from closed thin loop to gradually saturated loop with decreasing temperature.

When the Bi^{3+} concentration is above 10 mol%, we can see that the permittivity over the whole temperature range decreases without further shift in peak temperature, and the peak became more diffused. These compositions are believed to be relaxor. It should be attributed to the fact that interaction among polar nanoregions dominates the whole lattice and the primary long-range order structure has almost been destructed absolutely. So ferroelectric behavior vanishes and relaxor behavior dominates.

In the previous articles [18], relaxation properties of compositionally disordered ABO_3 perovskites, which were usually quantum paraelectrics, such as $KTaO_3(Mn,Fe,Ni,Co$ [23, 24]), $SrTiO_3(Ca$ [25]), were studied. Among all these substitutes, the phenomenon is that in the very dilute limit (<1 mol%), each polar domain behaves as a noninteracting dipolar entity with a single relaxation time, just like our results below 1 mol%. At higher concentration of disorder, the polar domains can interact leading to more complex relaxation behavior with distribution of relaxation times. The manifestation of such behavior is the formation of a glass-like relaxor state, or even an order FE state for a sufficiently high concentration of overlapping domains. This view is fit for a large number of systems, including our system. However, the difference is that our matrix-system is a ferroelectric ABO_3 perovskite with long-range order structure. When polar regions are interacting, they destruct the primary long-range order at the same time. Furthermore, the influence of impurity in ferroelectric matrix is to dissolve the ferroelectricity as well as to form relaxor behavior.

Summary

$(Ba_{0.6}Sr_{0.4})_{1-1.5x}Bi_xTiO_3$ $(0 \leq x \leq 0.20)$ ceramics were synthesized, and their microstructure and crystal structure were studied. The limit of solid solubility of Bi ions is identified as about $x = 0.10$ by XRD, SEM, and lattice constant measurement.

The dielectric behavior in this doped system described the transition from ferroelectric to relaxor ferroelectric and then to relaxor. Hysteresis loops, thermal expansion and dielectric tunability demonstrated the process from different aspects. The variation of properties was attributed to the interaction between the impurity induced polar regions and former long-order structure.

References

1. Sengupta LC, Sengupta S (1997) IEEE Trans Ultrason Ferrolectr Freq Control 44:792
2. Gevorgian SS, Kollgerg EL (2001) IEEE Trans Microwave Theory Technol 49:2117
3. Hwang CS, Park SO, Cho HJ, Kang CS, Kang HK, Lee SI, Lee MY (1995) Appl Phys Lett 67:2819
4. Liu S, Liu M, Zeng Y, Li C, Chen S, Huang Y, Xia D (2002) Mater Sci Eng C 22:73
5. Tanaka A (1996) IEEE Trans Electron Devices 43:1844
6. Cole MW, Hbbard C, Ngo E, Ervin M, Wood M, Geyer RG, (2002) J Appl Phys 92:475
7. Kang KT, Lim MH, Kim HG, Choi YW, Tuller HL, Kim D, Hong JM (2005) Appl Phys Lett 87:242908
8. Saha S, Krupanidhi SB (2001) J Appl Phys 90:1250
9. Wang SY, Cheng BL, Wang C, Dai SY, Lu HB, Zhou YL, Chen ZH, Yang GZ (2004) Appl Phys Lett 84:4116
10. Jeon YA, Seo TS, Yoon SG (2001) Jpn J Appl Phys Part 1 40:6496
11. Radhapiyari L, James AR, Thakur OP, Prakash C (2005) Mater Sci Eng B 117:5
12. Sun X, Zhu B, Liu T, Li M, Zhao X, Wang D, Sun C, Chan HLW (2006) J Appl Phys 99:084103
13. Cole MW, Joshi PC, Ervin MH (2001) J Appl Phys 89:6336
14. Kim KT, Kim CI (2003) Microelectron Eng 66:835
15. Zhou L, Vilarinho PM, Baptista JL (2001) J Eur Ceram Soc 21:531
16. Chen W, Yao X, Wei X (2007) Solid State Commun 141:84
17. Yun S, Wang X (2006) Mater Lett 60:2211
18. Samara GA (2003) J Phys Condens Matter 15:367
19. Burns G, Dacol FH (1983) Phys Rev B 28:2527
20. Burns G, Dacol FH (1983) Solid State Commun 48:853
21. Burns G, Dacol FH (1984) Phys Rev B 30:4012
22. Chong KB, Kong LB, Chen L (2004) J Appl Phys 95:1416
23. Laguta VV, Glinchuk MD, Bykovi P, Rosa U, Jsastrabik L, Savinov M, Trybula Z (2000) Phys Rev B 61:3897
24. Nowick AS, Fu SQ, Lee WK, Lin BS, Scherban T (1994) Mater Sci Eng B 23:19
25. Kleemann W, Albertini A, Kuss M, Lindner R (1997) Ferro-electrics 203:57